

Article

Prediction of Post-Intubation Tachycardia Using Machine-Learning Models

Hanna Kim ^{1,†} , Young-Seob Jeong ^{1,†} , Ah Reum Kang ¹ , Woohyun Jung ² ,
Yang Hoon Chung ² , Bon Sung Koo ²  and Sang Hyun Kim ^{2,*} 

¹ SCH Media Labs, Soonchunhyang University, Asan 31538, Korea; hanna@sch.ac.kr (H.K.);
bytecell@sch.ac.kr (Y.-S.J.); armk@arkang.net (A.R.K.)

² Department of Anesthesiology and Pain Medicine, Soonchunhyang University Bucheon Hospital,
Soonchunhyang University College of Medicine, Bucheon 14584, Korea; mulungtomato@naver.com (W.J.);
drcyh79@schmc.ac.kr (Y.H.C.); kbs0803@schmc.ac.kr (B.S.K.)

* Correspondence: skim@schmc.ac.kr; Tel.: +82-32-621-5328; Fax: +82-32-621-5322

† These authors contributed equally to this work.

Received: 31 December 2019; Accepted: 3 February 2020; Published: 8 February 2020



Abstract: Tachycardia is defined as a heart rate greater than 100 bpm for more than 1 min. Tachycardia often occurs after endotracheal intubation and can cause serious complication in patients with cardiovascular disease. The ability to predict post-intubation tachycardia would help clinicians by notifying a potential event to pre-treat. In this paper, we predict the potential post-intubation tachycardia. Given electronic medical record and vital signs collected before tracheal intubation, we predict whether post-intubation tachycardia will occur within 10 min. Of 1931 available patient datasets, 257 remained after filtering those with inappropriate data such as outliers and inappropriate annotations. Three feature sets were designed using feature selection algorithms, and two additional feature sets were defined by statistical inspection or manual examination. The five feature sets were compared with various machine learning models such as naïve Bayes classifiers, logistic regression, random forest, support vector machines, extreme gradient boosting, and artificial neural networks. Parameters of the models were optimized for each feature set. By 10-fold cross validation, we found that an logistic regression model with eight-dimensional hand-crafted features achieved an accuracy of 80.5%, recall of 85.1%, precision of 79.9%, an F1 score of 79.9%, and an area under the receiver operating characteristic curve of 0.85.

Keywords: tachycardia prediction; tracheal intubation; electronic medical record; vital sign; machine learning; clinical decision support

1. Introduction

The usual circulatory response to laryngeal and tracheal stimulation during tracheal intubation in anesthetized patients are tachycardia and a rise in arterial pressure due to reflex sympathetic stimulation [1–3]. The resulting tachycardia is transient and poses little risk to healthy patients. However, in patients with cardiovascular disease, it can induce a cardiac oxygen imbalance and cause serious complications such as myocardial ischemia. To prevent such tachycardia, β -blockers, lidocaine, opioids, and deep anesthesia are used [4–6]. These methods do not always effectively block tachycardia and the potential for complications associated with drug administration cannot be ignored. If post-intubation tachycardia can be predicted, pre-intubation medication could be administered prior to intubation to mitigate the degree of tachycardia. However, several characteristics of anesthesia induction make prediction difficult. Patients often experience anxiety prior to surgery, which activates the sympathetic system. Medication (e.g., β -blockers) and preexisting medical

conditions (e.g., cardiovascular diseases, diabetes) are confounding factors. Furthermore, bolus administration of anesthesia induction agents responds variously according to the patient's general condition and existing disease. Tracheal intubation itself causes various hemodynamic responses, further complicating the task of predicting such responses. With the universal use of electronic medical records (EMR; otherwise referred to as Electronic Healthcare Records) and real-time biological signal collection equipment, data from EMR (e.g., patient demographic information, coexisting disease, and medication history) and physiological and pharmacological data obtained from various anesthesia monitoring devices can be collected simultaneously during anesthesia and surgery. The development of machine learning has reached a stage where it may be possible to train systems to predict blood-pressure fluctuation during anesthesia [7]. However, to our knowledge, no studies have yet predicted the occurrence of tachycardia after induction of anesthesia by machine learning.

Although no studies of predictive systems for post-intubation tachycardia have been conducted, reports on related events (e.g., ventricular tachycardia, cardiac arrest, and arrhythmia) are available. In most studies, the related events were predicted using heart rate variability (HRV) as the main variable and several have adopted machine learning models such as logistic regression (LR), random forest (RF), decision tree (DT), artificial neural networks (ANN) [8–11]. Some studies have investigated feature selection algorithms to enhance model performance and identify indicative features. Riasi et al. [12] used a linear correlation method to predict ventricular tachycardia (VT). They analyzed the linear correlation of the features, removed highly correlated features, and achieved a sensitivity of 0.88 using support vector machines (SVMs). Yaghouby et al. [13] used generalized discriminant analysis (GDA) feature reduction to predict four types of cardiac arrhythmias. A total of nine linear and nonlinear features were extracted from the HRV signals, which were reduced to three-dimensional values by GDA. Feature selection improved accuracy rates by between 1% and 7%, and they achieved an accuracy of 100% with an ANN model. As feature selection has shown its potential to resolve a variety of complex relationships between factors (or features), we employed feature selection algorithms to deal with factors that affect the heart rate after intubation. Among the known factors are patient characteristics (e.g., age, comorbidity), a history of taking cardiovascular drugs before surgery (e.g., β -blockers, calcium channel blockers, antiarrhythmics), time to intubation, degree of muscle relaxation, intubation methods (e.g., traditional direct laryngoscope, video laryngoscope), and the type and amount of anesthesia drug injected. We also designed feature sets based on statistical clues (e.g., *p*-value) and manual examination. We applied these carefully designed features to machine learning models for tachycardia prediction.

In this paper, we aimed to predict whether post-intubation tachycardia will appear within 10 min, given EMR and vital signs collected before tracheal intubation. Tachycardia is defined a heart rate greater than 100 bpm for more than 1 min. As far as we know, this is the first study to predict tachycardia after tracheal intubation. To predict tachycardia, we used a variety of machine learning models with feature selection techniques. We believe that this will prove helpful for clinicians by notifying a potential event to pre-treat.

This paper is structured as follows. Section 2 describes the characteristics of the data and preprocessing steps. It also supplies details on how we used feature selection algorithms and machine learning models. Section 3 provides details of experimental settings and results, Section 4 discusses about the results, and Section 5 concludes the paper.

2. Materials and Methods

2.1. Data Preparation

Datasets were collected from nine operating rooms at Soonchunhyang University Bucheon Hospital, Bucheon city, Republic of Korea, between 29 October 2018, and 30 September 2019. The data were collected from patients who had received total intravenous anesthesia (TIVA), and were at least

18 years old. The datasets do not contain any direct patient identifiers and additional approval from our institutional review board was obtained for this retrospective study (No. 2019-10-024-002).

The datasets consisted of electronic medical records (EMRs) and vital signs. The EMR data were manually collected and included age, sex, height, weight, body mass index (BMI), American Society of Anesthesiologists (ASA) physical status grade, and types of coexisting diseases. Vital signs were collected automatically between the time of entering the operating room and the beginning of operation. Vital signs were collected using a Vital Recorder [14] connected to several devices in operating rooms: Bx50 (patient monitor), Solar 8000M (patient monitor), Datex-Ohmeda (anesthesia machine), Primus (anesthesia machine), BIS (brain monitor) and Orchestra (infusion pump). Vital signs included 35 variables such as heart rate (HR), systolic blood pressure (SBP), tidal volume (TV), carbon dioxide (CO2), end-tidal CO2 partial pressure (ETCO2), positive endexpiratory pressure (PEEP), bispectral index (BIS), and so forth. Figure 1 shows a sample of the two types of data; the EMR is collected once for each operation, whereas the vital signs are supposed to be gathered every second continuously. Figure 1 shows a sample of the two types of data; the EMR data were collected once for each operation, whereas vital signs were ideally gathered every second continuously. Details of the two types of data are summarized in Table 1, where the baseline vital values are collected only before anesthesia induction.

Case ID	Sex	Age	Weight	Height	BMI	ASA	Hypertension	Atrial fibrillation	Angina	Dementia
.....
20_191223_XXXXX	F	27	47	163	17.69	1	0	0	1	0
.....

(a) EMR data

20_191223_XXXXX									
Time	HR	NIBP_S	ETCO2	CO2	BIS/BIS	NMT_TOF_CNT	PROPOFOL_CE	EVENT
.....
00:06:59	95	110	1.2	2.4	78	2	3.135	-
00:07:00	95	122	1.2	2.4	77	2	3.135	-
00:07:01	98	122	2.8	0	69	0	3.155	-
.....
00:07:59	96	122	3	0	65	0	3.38	-
00:08:00	96	124	3	0	68	0	3.38	-
00:08:01	97	124	3.4	3.7	67	1	3.459	-
00:08:02	97	124	3.4	3.7	68	1	3.459	intubation
.....
00:12:00	101	141	4.9	4.4	80	3	4.04	-
00:12:01	100	141	4.1	4.6	81	1	4.067	-
00:12:02	100	141	4.1	4.6	78	1	4.067	-
00:12:03	100	141	4.1	4.6	74	1	4.067	-
00:12:04	100	141	3.2	0	68	0	4.436	-
.....	-

(b) Vital signs

Figure 1. (a) Sample EMR data, and (b) sample vital signs of a patient.

Table 1. Description of collected data.

Source	Category	Feature Name
Electronic medical record	Demographic data	Age Sex Height Weight Body mass index ASA classification
	Comorbidities	Cardiovascular disease Respiratory disease Coronary artery disease Gastrointestinal disease Renal disease Endocrine disease Neurologic disease
Vital recorder	Baseline	Heart rate Systolic blood pressure Mean blood pressure Diastolic blood pressure
	Noninvasive blood pressure	Systolic blood pressure Mean blood pressure Diastolic blood pressure
	Heart rate	Heart rate
	Mechanical ventilation data	Tidal volume Minute ventilation Respiratory rate Mean positive airway pressure Peak inspiratory pressure End-tidal CO2 partial pressure Carbon dioxide Saturation of partial pressure of oxygen Positive endexpiratory pressure
	Neuromuscular transmission	train-of-four count
	Bispectral index	Spectral edge frequency Signal quality index Electromyogram power Total power Bispectral index value
	Anesthetic drug - propofol - remifentanyl	Volume Rate Plasma concentration Effect-site concentration Target concentration
	Vasoactive drug administration - Ephedrine - Phenylephrine - Esmolol - Nicardipine - Dexamethasone	Volume
	Muscle relaxant - Rocuronium	Volume

The datasets required preprocessing because of missing values (e.g., signal quality index (SQI) of BIS), inconsistent sampling rates, outliers (e.g., height), and incorrect time-logs of intubation. Missing values from the BIS were replaced by the mean of the surrounding values. Other missing values were replaced by the last observed values. Different vital signs had inconsistent sampling rates; for example, generally noninvasive blood pressure was recorded every minute, whereas the respiratory rate was recorded every 3 s. To handle this, as the fastest sampling rate was 1 s, we assume that all vital signs had the same sampling rate of 1 s. If a sampling rate of a particular variable was 3 s, then the corresponding variable values were copied twice.

After the missing values and inconsistent sampling rates were addressed, it was necessary to filter some data as depicted in Figure 2. Of the original 1931 patients collected between 29 October 2018, and 30 September 2019, both vital signs and EMR were available for only 1093. Outlier values (e.g., height of 1554.2 cm, remifentanyl volume of 538,976.25 µg) as determined by a predefined range of variables were removed. The patients without BIS, neuromuscular transmission train-of-four count (NMT_TOF_CNT), or CO₂ were filtered out. The patients without any intubation annotation (i.e., “EVENT”) were also removed because our purpose was to predict post-intubation tachycardia. Furthermore, because the intubation annotation may have been wrong for several reasons, we designed Algorithm 1 to correct wrong annotations. The algorithm also found patient data that could not be corrected, and 271 were discarded. Based on the corrected annotations of intubation, we filtered 64 patients data of two cases: (1) intubation only 10 s after anesthesia induction, and (2) operation begins within 10 min after intubation.

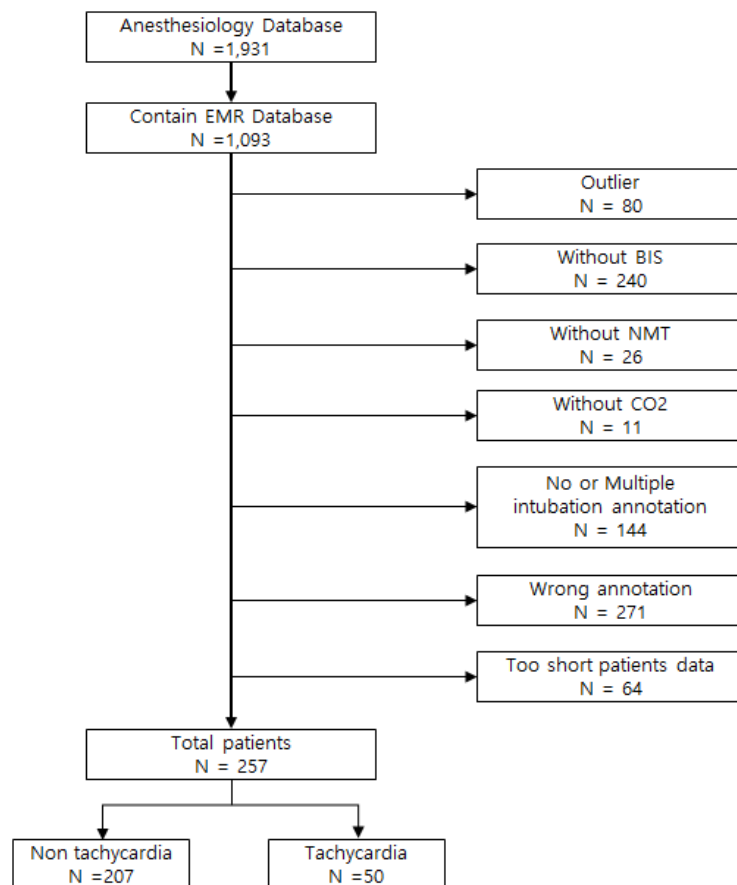


Figure 2. Data filtering.

The major purpose of Algorithm 1 was to correct annotations of intubation. The time-step (or point) of tracheal intubation was annotated manually by the perioperative nurse (or anesthesiologist) in the operating room. Therefore, the annotated points may have been incorrect for several reasons

(e.g., a mistake or delay). For example, the EVENT column of Figure 1b has the incorrect annotation “intubation” at 00:08:02, because the CO₂ value must remain at zero during tracheal intubation. Our purpose was to predict post-intubation tachycardia, so it was critical to find the correct intubation points. Algorithm 1 describes four steps of finding the start and end points of tracheal intubation. More formally, in Figure 3, the algorithm identifies the beginning point of intubation I_s and the ending point of intubation I_e .

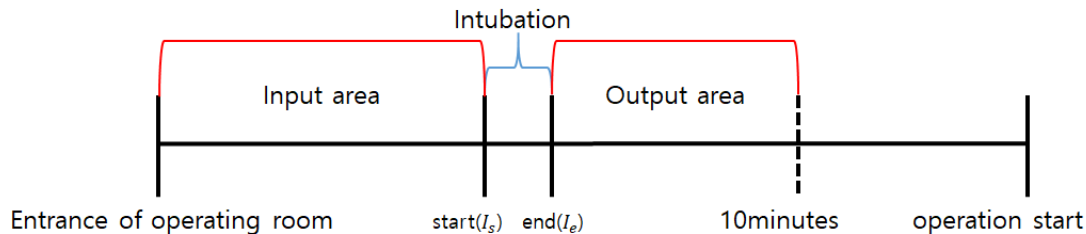


Figure 3. Input and output area based on the intubation points.

The first step of Algorithm 1 was to find candidate points of tracheal intubation using three conditions, as shown in line 4. The first condition checked if the bispectral index value (BIS) was lower than 70. When patients entered the operating room, TIVA using propofol and remifentanyl via a target controlled infusion pump (Orchestra Base Primea with module DPS; Fresenius Kabi AG, Germany) was administered. After anesthesia, patients gradually lost consciousness as BIS decreased. In Figure 1b, this condition is met at 00:07:01. The second condition checks muscle state; neuromuscular transmission train of four count (NMT_TOF_CNT) is 0 or 1 when the muscle is relaxed. The rocuronium was injected intravenously, and we electrically stimulated the nerves dominating the patient’s thumb and measured their movements to determine if the muscles were relaxed. The last condition checks if the carbon dioxide (CO₂) values for 10 s remain at zero. After receiving the muscle relaxant, the patients could not breathe on their own, so CO₂ values were zero. In Figure 1b, the annotated event “intubation” violates this condition, meaning that the annotation must be incorrect. By the above three conditions, the first step finds a candidate set of beginning points of intubation. For example, the candidate set included the point 00:07:01 in Figure 1b. If no candidate was found, then the corresponding data were discarded, as described in line 12. The lines between 14 and 18 were to take only the first candidate point if some candidate points are consecutive; for example, given four candidate points [10, 20, 30, 50], the two points 20 and 30 were to be filtered out, resulting in two remaining candidate points [10, 50].

The second step of the algorithm was to find a manually annotated intubation point in the operating room. Unless there was only one annotated intubation point, the corresponding data were discarded. In other words, if there were multiple annotated points or no points at all, then the corresponding data were regarded as incorrect. Such wrong data were discarded even multiple candidate points CI_s were obtained from step 1, which means that the CI_s and MI were required to find the intubation points I_s and I_e in the following steps. The third step was to find the beginning point I_s . The I_s was found by comparing MI and multiple candidate points CI_s . By comparing the difference of MI with each element of CI_s , the nearest element of CI_s to MI became I_s . For example, in Figure 1b, assume that CI_s and MI are [00:07:01, 00:12:04] and [00:08:02], respectively. The I_s will be 00:07:01 because it is the nearest candidate point to 00:08:02. The last step was to find the ending point I_e of intubation. It assumes that the post-intubation CO₂ emission was greater than the pre-intubation CO₂ emission. For example, in Figure 1b, the $CO_{2_{pre}}$ will be 2.4 at 00:07:00. The I_e will be 00:08:01 because it is the earliest point with a greater CO₂ value than $CO_{2_{pre}}$. If the I_e was not found by this step, then the corresponding data were to be discarded; but we did not observe such a case.

Algorithm 1: Finding the start and end points of tracheal intubation for a target patient.

Result: Beginning point of intubation I_s , Ending point of intubation I_e

- 1 **STEP 1:** Finding a set of candidates for beginning points of tracheal intubation
Output: Candidates of beginning point CI_s
- 2 Timestep $i \leftarrow 0$; $CI_s \leftarrow \{\}$
- 3 **for** i -th point **do**
- 4 **if** $BIS[i] < 70$ **and** $(NMT_TOF_CNT[i] == 0$ **or** $1)$ **and** $CO2[i:i+10] == 0$ **then**
- 5 $CI_s.append(i)$
- 6 $i \leftarrow i + 10$
- 7 **else**
- 8 $i \leftarrow i + 1$
- 9 **end**
- 10 **end**
- 11 **if** $len(CI_s) == 0$ **then**
- 12 discard this patient data
- 13 **else**
- 14 **for** each pair (ci_1, ci_2) in $reverse(CI_s)$ **do**
- 15 **if** $ci_1 - ci_2 \leq 10$ **then**
- 16 $CI_s.remove(ci_1)$
- 17 **end**
- 18 **end**
- 19 **end**
- 20 **STEP 2:** Finding manually tagged intubation point in the operating room
Output: Manually tagged intubation point MI
- 21 Timestep $i \leftarrow 0$; $MI \leftarrow NULL$; $MI_c \leftarrow \{\}$
- 22 **for** i -th point **do**
- 23 **if** $EVENT[i] == 'intubation'$ **then**
- 24 $MI_c.append(i)$
- 25 $i \leftarrow i + 1$
- 26 **end**
- 27 **end**
- 28 **if** $len(MI_c) != 1$ **then**
- 29 discard this patient data
- 30 **else**
- 31 $MI \leftarrow MI_c[0]$
- 32 **end**
- 33 **STEP 3:** Finding the beginning point of intubation
Output: Beginning point of intubation I_s
- 34 $I_s = \operatorname{argmin}_{ci \in CI_s} \|MI - ci\|$
- 35 **STEP 4:** Finding the ending point of intubation
Output: Ending point of intubation I_e
- 36 Pre-intubation $CO2_{pre} \leftarrow CO2[I_s-1]$
- 37 **for** i -th point $> I_s$ **do**
- 38 **if** $CO2_{pre} < CO2[i]$ **then**
- 39 $I_e = i$
- 40 break
- 41 **end**
- 42 **end**

2.2. Feature Selection

Our purpose was to predict a post-intubation tachycardia, for which the input feature was obtained from the “input area” in Figure 3, and the output was 1 (or true) if the tachycardia occurred in the “output area”; otherwise it was 0 (or false). In this paper, tachycardia is defined as a HR greater than 100 bpm for more than 1 min. The input feature is defined using two types of data (e.g., EMR and vital signs). First, a 24-dimensional feature vector f_{EMR} was obtained from EMR, including age, sex, BMI, and so forth; details of the 24-dimensional feature can be found in the first two rows of Table A1 in the Appendix. For example, if the patient was female and had a cardiovascular disease (e.g., hypertension), then f_{EMR} was $[\dots, f_{sex} = 1, \dots, f_{hypertension} = 1, \dots]$. Second, a 129-dimensional feature vector f_{vital} was obtained from the vital signs. The f_{vital} contains mainly min, max, mean, and standard deviation (sd) of each vital sign; details can be found in Table A1 of the Appendix. For example, if systolic blood pressure (SBP) of the baseline was 130 and the minimum value of respiratory rate (RR) was 4.9, then f_{vital} was $[\dots, f_{baseSBP} = 130, \dots, f_{minRR} = 4.9, \dots]$. The two feature vectors f_{EMR} and f_{vital} were merged into a 153-dimensional feature vector f_{input} . Every numerical element of the f_{input} was normalized between 0 and 1.

Feature selection finds a promising set of features that has a potential to contribute performance improvement. Feature selection is known to shorten training time, reduce overfitting, and improve accuracy [15]. It has produced useful results for ventricular tachycardia and arrhythmia in previous studies [12,13]. We compared feature selection with three different measurements: recursive feature elimination (RFE), Gini index (GI), and a univariate statistical test (UST) using mutual information. The RFE and GI-based feature selection were performed with a random forest (RF) classifier using scikit-learn [16]. By grid searching, RFE, GI, and UST-based feature selection resulted in 10, 15, and 15 promising feature sets, respectively. Details of the selected features are listed in Table 2.

In addition to feature selection with the three measurements, we also prepared two additional feature sets: a *p*-value based feature set and a manually designed feature set. In Table 2, the “*P*-based” and “Hand-crafted” feature sets indicate the two feature sets, respectively. The *P*-based feature set was defined by statistical clues; we conducted a t-test or Wilcoxon test for continuous variables (e.g., height, tidal volume), and chi-squared or Fisher tests for categorical variables (e.g., sex, ephedrine). We observed significant statistical differences in baseline heart rate, noninvasive heart rate, and remifentanyl values, as shown in Table 3. However, the hand-crafted feature set was carefully designed through an exploratory data analysis process. That is, by manually examining a group of patients, we picked eight promising features, including sex, HR_mean, remifentanyl_CE_max, remifentanyl_CP_max, remifentanyl_VOL_max, remifentanyl_VOL_mean, BIS_min, and MV_max.

Table 2. Feature sets.

All 153 Features	RFE-Based	GI-Based	UST-Based	P-Based	Hand-Crafted
Sex					•
Comorbidities - no.					
Endocrine disease					
Hemoglobin A1c			•		
Baseline					
Heart rate			•	•	
Heart rate					
Min	•	•	•		
Max	•	•	•		
Mean	•	•	•	•	•
Sd	•				
Difference Heart rate					
Max		•			
Mean		•			
Mechanical ventilation data					
Minute ventilation					
Max		•			•

Table 2. Cont.

All 153 Features	RFE-based	GI-based	UST-based	P-based	Hand-Crafted
End-tidal CO2 partial pressure					
Max			•		
Mean	•				
Carbon dioxide					
Mean		•			
PLETH_SPO2					
Mean	•				
Positive endexpiratory pressure					
Sd		•			
Bispectral Index					
Spectral frequency					
Mean		•			
Signal quality index					
Sd			•		
Electromyography					
Min		•			
Mean			•		
Total power					
Max		•			
Mean	•	•			
Bispectral index value					
Min			•		•
Max			•		
Sd	•				
Anesthetic drug					
Volume					
Propofol					
Min		•			
Remifentanil					
Max					•
Mean				•	•
Rate					
Propofol					
Mean		•	•		
Sd	•				
Plasma concentration					
Remifentanil					
Max	•		•		•
Effect-site concentration					
Propofol					
Min		•			
Remifentanil					
Max					•
Mean			•		
Pre-intubation sinus tachycardia					
Occurrence			•		
Frequency			•		

RFE stands for recursive feature elimination, GI means Gini index, UST implies univariate statistical test, and P-based represents *p*-value based feature sets, and PLETH_SPO2 means saturation of partial pressure of oxygen.

Table 3. Statistical characteristics of variables.

	All Cases (n = 257)	No Tachycardia (n = 207)	Tachycardia (n = 50)	p Value
Age - yr	58.2 (14.5)	58.7 (14.2)	56.2 (15.7)	0.266
Sex (Female)	131 (51.0%)	106 (51.2%)	25 (50.0%)	0.878
Height—cm	161.2 (9.3)	161.2 (9.4)	161.5 (9.3)	0.851
Weight—kg	64.6 (12.4)	64.7 (12.3)	64.1 (12.8)	0.777
BMI—kg/m ²	24.7 (3.5)	24.8 (3.5)	24.5 (3.7)	0.588
ASA classification - no.				0.647
1	72 (58.8%)	59 (28.5%)	13 (26.0%)	
2	151 (28.0%)	119 (57.5%)	32 (64.0%)	
3	34 (13.2%)	29 (14.0%)	5 (10.0%)	
Comorbidities - no.				
Cardiovascular disease				
Hypertension	100 (38.9%)	81 (39.1%)	19 (38.0%)	0.883
Atrial fibrillation	6 (2.3%)	4 (1.9%)	2 (4.0%)	0.331
Coronary artery disease	11 (4.3%)	9 (4.3%)	2 (4.0%)	0.636
Angina pectoris	5 (1.9%)	5 (2.4%)	0 (0.0%)	0.336
Congestive heart failure	2 (0.8%)	1 (0.5%)	1 (2.0%)	0.352
Respiratory disease				
Asthma	12 (4.7%)	8 (3.9%)	4 (8.0%)	0.187
Chronic obstructive pulmonary disease	4 (1.6%)	4 (1.9%)	0 (0.0%)	0.418
Gastrointestinal disease				
Hepatitis	3 (1.2%)	2 (1.0%)	1 (2.0%)	0.479
Liver cirrhosis	7 (2.7%)	6 (2.9%)	1 (2.0%)	0.591
Viral carrier	7 (2.7%)	5 (2.4%)	2 (4.0%)	0.409
Hepatitis B viral infection	14 (5.4%)	10 (4.8%)	4 (8.0%)	0.280
Renal disease				
Chronic kidney injury				0.574
2	1 (0.4%)	1 (0.5%)	0 (0.0%)	
3	6 (2.3%)	6 (2.9%)	0 (0.0%)	
4	1 (0.4%)	1 (0.5%)	0 (0.0%)	
End-stage renal disease	2 (0.8%)	2 (1.0%)	0 (0.0%)	0.648
Endocrine disease				
Diabetes mellitus	58 (22.6%)	50 (24.2%)	8 (16.0%)	0.216
Thyroid disease				0.386
1	3 (1.2%)	3 (1.4%)	0 (0.0%)	
2	2 (0.8%)	1 (0.5%)	1 (2.0%)	
3	13 (5.1%)	9 (4.3%)	4 (8.0%)	
Hemoglobin A1c	1.5 (2.9%)	1.6 (3.0%)	1.0 (2.4%)	0.223
Neurologic disease				
Cerebrovascular disease	10 (3.9%)	8 (3.9%)	2 (4.0%)	0.612
Dementia	1 (0.4%)	1 (0.5%)	0 (0.0%)	0.805
Baseline				
Systolic blood pressure—mmHg	142.8 (23.7)	143.3 (24.7)	141.0 (19.3)	0.546
Mean blood pressure—mmHg	102.7 (15.8)	102.6 (16.4)	102.8 (13.0)	0.959
Diastolic blood pressure—mmHg	78.5 (11.5)	77.9 (11.4)	80.8 (11.6)	0.11
Heart rate—/min	75.5 (15.6)	73.3 (14.5)	84.6 (17.1)	< 0.001 ***
Noninvasive blood pressure—mmHg				
Systolic	123.4 (19.6)	123.7 (20.2)	122.0 (16.8)	0.57
Mean	123.4 (19.6)	123.7 (20.2)	122.0 (16.8)	0.57
Diastolic	69.9 (9.6)	69.6 (9.8)	71.0 (8.7)	0.357
Heart rate—/min	72.9 (12.6)	70.1 (10.9)	84.4 (12.8)	< 0.001 ***

Table 3. Cont.

	All Cases (n = 257)	No Tachycardia (n = 207)	Tachycardia (n = 50)	p Value
Mechanical ventilation data				
Tidal volume—mL	239.4 (86.0)	237.1 (85.7)	248.8 (87.4)	0.39
Minute ventilation—L/min	3.8 (1.5)	3.8 (1.5)	4.1 (1.5)	0.131
Respiratory rate—/min	15.9 (5.8)	15.6 (5.8)	16.9 (5.6)	0.169
Mean positive airway pressure—cmH2O	6.8 (1.9)	6.8 (1.9)	6.9 (1.8)	0.645
Peak inspiratory pressure—cmH2O	14.8 (4.3)	14.8 (4.2)	14.6 (4.4)	0.783
End-tidal CO2 partial pressure—%	22.8 (0.7)	2.8 (0.7)	2.8 (0.5)	0.567
Carbon dioxide—%	1.1 (0.4)	1.1 (0.4)	1.1 (0.3)	0.977
Saturation of partial pressure of oxygen—%	99.1 (1.2)	99.0 (1.2)	99.1 (1.0)	0.635
Positive endexpiratory pressure—cmH2O	2.7 (1.1)	2.7 (1.1)	2.8 (1.2)	0.334
Neuromuscular transmission				
train-of-four count	1.5 (0.6)	1.5 (0.6)	1.5 (0.7)	0.838
Bispectral Index				
Spectral frequency—Hz	17.5 (2.6)	17.4 (2.5)	18.0 (2.9)	0.195
Signal quality index—Hz	81.0 (12.0)	81.0 (12.0)	81.2 (12.1)	0.902
Electromyography—Hz	35.4 (4.2)	35.3 (4.2)	35.9 (4.0)	0.331
Total power	63.9 (2.9)	63.8 (2.7)	64.2 (3.4)	0.479
Bispectral index value	63.2 (10.9)	62.8 (10.6)	65.0 (12.1)	0.185
Anesthetic drug				
Volume				
Propofol—mg	112.7 (31.3)	112.6 (30.8)	113.2 (33.2)	0.909
Remifentanil—μ g	32.7 (15.7)	34.0 (16.3)	27.4 (11.8)	0.001***
Rate - mL/hr				
Propofol	200.3 (184.5)	208.9 (194.0)	164.8 (134.8)	0.062
Remifentanil	44.0 (81.2)	44.4 (84.0)	42.0 (69.1)	0.852
Plasma concentration				
Propofol—mcg/mL	6.0 (1.6)	6.0 (1.7)	6.0 (1.3)	0.947
Remifentanil—ng/mL	2.7 (1.6)	2.8 (1.7)	2.2 (1.2)	0.017*
Effect-site concentration				
Propofol—mcg/mL	4.2 (0.8)	4.2 (0.8)	4.3 (0.7)	0.471
Remifentanil—ng/mL	1.5 (0.7)	1.5 (0.7)	1.3 (0.6)	0.04*
Target concentration				
Propofol—mcg/mL	4.9 (0.8)	4.8 (0.8)	5.0 (0.8)	0.275
Remifentanil—ng/mL	1.8 (0.9)	1.9 (0.9)	1.6 (0.8)	0.035 *
Vasoactive drug administration - no.				
Ephedrine	3 (1.2%)	3 (1.4%)	0 (0.0%)	0.521
Phenylephrine	3 (1.2%)	3 (1.4%)	0 (0.0%)	0.521
Esmolol	2 (0.8%)	1 (0.5%)	1 (2.0%)	0.352
Nicardipine	1 (0.4%)	1 (0.5%)	0 (0.0%)	0.805
Dexamethasone	68 (26.5%)	57 (27.5%)	11 (22.0%)	0.426
Muscle relaxant				
Rocuronium—mg	46.2 (11.9)	45.8 (12.4)	48.0 (9.3)	0.239

Continuous variable are expressed as mean and standard deviation. T-test or Wilcoxon test was performed appropriately. For categorical variables, numbers and ratios are displayed, and chi-square tests or Fisher's tests performed appropriately. * 0.05, *** 0.001.

The five feature sets were compared using various machine learning models: random forest (RF) [17], logistic regression (LR) [18], naïve Bayes classifiers (NB) [19], support vector machine (SVM) [20], extreme gradient boosting (XGB) [21], and artificial neural networks (ANN) [22]. The ANN had two hidden layers, in which the first and second layers had 15 and 20 nodes, respectively.

3. Results

Among the 257 patients, there were positive patients that had the post-intubation tachycardia, where the number of positive patients $|D_{pos}| = 50$. To avoid such imbalance, we randomly divided the remaining 207

negative patients D_{neg} into four disjoint subsets, where $|D_{neg^1}| = 52$, $|D_{neg^2}| = 52$, $|D_{neg^3}| = 52$, and $|D_{neg^4}| = 51$. We conducted four independent experiments with every pair of D_{pos} and $\{D_{neg^1}, D_{neg^2}, D_{neg^3}, D_{neg^4}\}$; the total amount of datasets for the four experiments was 102, 102, 102, and 101, respectively. All experimental results were averaged values of 10-fold cross-validation. The performance of different models was compared by accuracy, precision, recall, and F1 score [23]. We also utilized an area under the receiver operating characteristic curve (AUC) to compare the models; larger AUC values implied better models.

We applied our five feature sets to six machine learning models. Parameters of each model were optimized through a grid search, for which the settings are described in Table 4. We used a computer with eight Central Processing Units (CPU) of i7-7700 3.6 GHz and two NVIDIA GeForce 1080 Ti. The machine learning models were implemented with Python3 language.

Table 4. Parameter settings for machine learning models.

Models	Description
Artificial neural network	Common parameter : Activation (relu), Solver (adam), L2 penalty (0.001), Maximum iteration (200)
	Common structure : two hidden layers = [15, 20]
	All feature : L2 penalty = 0.1, One hidden layer with 10 nodes
	RFE-based : Initial parameter
	GI-based : Initial parameter
	UST-based : Activation = identity, Solver = sgd P-based : Activation = identity, Solver = lbfgs Hand-crafted : Activation = identity, Solver = lbfgs
Logistic regression	Common parameter : Penalty (L2), C (1.0), Solver (liblinear)
	All feature : Penalty = L1, C = 0.1
	RFE-based : Penalty = L1
	GI-based : Penalty = L1
	UST-based : Penalty = L1
	P-based : C=10 Hand-crafted : Initial parameter
Naive Bayes (GaussianNB)	Naive Bayes using Gaussian distribution
Random forest	Common parameter : # of estimators (10), Maximum depth (None), n_jobs (None)
	All feature : # of estimators = 30, Maximum depth = 2, n_jobs = -1
	RFE-based : # of estimators = 700, Maximum depth = 7
	GI-based : # of estimators = 700, n_jobs = -1
	UST-based : # of estimators = 700
	P-based : Maximum depth = 2 Hand-crafted : Initial parameter
Support vector machines	Common parameter : Kernel (rbf), C (1.0), Maximum iteration (-1)
	All feature : Kernel = linear, C = 0.1
	RFE-based : Initial parameter
	GI-based : Kernel = linear
	UST-based : Initial parameter
	P-based : Kernel = linear Hand-crafted : Kernel = linear
Extreme gradient boosting	Common parameter : # of estimators (100), Gamma (0), n_jobs (1)
	All feature : # of estimators = 20
	RFE-based : Initial parameter
	GI-based : gamma = 0.1, n_jobs = -1
	UST-based : Initial parameter
	P-based : # of estimators = 20 Hand-crafted : Initial parameter

The experimental results are summarized in Table 5, where the first row, “All feature,” refers to a 153-dimensional feature vector f_{input} . The feature sets with feature selection algorithms (e.g., RFE-based, GI-based, and UST-based) gave better results than the f_{input} . Among the six machine learning models, LR and SVM achieved

the best accuracy of 80.5% with hand-crafted features. As it is more critical if we miss post-intubation tachycardia, better sensitivity is preferable. In terms of the sensitivity, the LR will be the most effective because its recall of tachycardia (85.1%) was greater than that of the SVM. As shown in Figure 4, the LR model achieved a much better AUC with the hand-crafted features than with the GI-based features. Although the hand-crafted feature was not the best for some models (e.g., random forest), all six models generally achieved high performances with it.

Table 5. Performance of machine learning models with different feature sets, where each precision, recall, and F1 score is a pair of two results for non-tachycardia(0) and tachycardia(1).

Feature Set	ANN	LR	NB	RF	SVM	XGB
All feature						
Accuracy	59.9	72.0	51.9	69.1	57.6	67.1
Precision(0/1)	59.4/60.7	67.7/71.4	51.7/52.5	65.0/72.2	57.7/55.7	66.7/66.2
Recall(0/1)	61.2/63.8	72.2/72.3	51.8/51.4	72.7/66.9	57.0/58.4	66.2/72.1
F1 score(0/1)	58.6/56.9	68.4/68.9	50.2/52.4	67.9/67.1	57.7/55.7	66.6/64.2
AUC	0.65	0.80	0.56	0.72	0.62	0.71
RFE-based feature						
Accuracy	69.6	71.8	70.3	74.2	71.8	71.5
Precision(0/1)	69.3/70.1	71.0/70.1	68.2/70.7	73.0/72.8	72.3/72.7	71.2/70.4
Recall(0/1)	67.7/75.8	69.3/75.9	73.4/71.8	71.8/78.3	73.1/75.7	68.2/77.0
F1 score(0/1)	69.2/67.8	69.7/69.1	68.5/66.6	72.2/72.2	69.6/68.8	68.9/69.6
AUC	0.79	0.79	0.79	0.79	0.81	0.78
GI-based feature						
Accuracy	70.1	71.0	69.3	71.1	68.8	73.5
Precision(0/1)	68.7/68.7	66.5/69.1	65.7/70.3	69.2/70.6	65.6/66.8	70.9/74.9
Recall(0/1)	68.4/72.3	66.0/74.4	71.6/70.2	72.4/72.9	65.1/72.8	76.5/73.6
F1 score(0/1)	66.7/67.0	68.4/69.1	68.2/66.2	68.3/67.7	67.2/66.4	70.9/70.1
AUC	0.76	0.78	0.76	0.77	0.74	0.79
UST-based feature						
Accuracy	71.6	72.1	66.4	73.2	66.1	70.8
Precision(0/1)	68.7/73.0	69.2/70.3	60.2/81.1	70.9/72.7	63.6/68.5	69.7/70.9
Recall(0/1)	72.9/72.3	70.3/73.2	87.7/45.0	74.1/74.1	71.3/63.9	73.4/69.5
F1 score(0/1)	68.7/68.8	68.2/70.4	71.3/60.1	70.3/69.5	66.4/61.0	70.5/67.2
AUC	0.80	0.79	0.78	0.79	0.74	0.79
P-based feature						
Accuracy	74.7	77.0	71.3	68.8	75.0	68.8
Precision(0/1)	72.3/73.8	74.3/75.3	66.4/75.2	64.6/67.5	72.3/75.5	67.4/68.5
Recall(0/1)	75.8/76.7	75.9/79.1	78.7/66.3	70.9/64.0	77.0/76.7	72.7/67.1
F1 score(0/1)	72.5/72.1	73.8/74.6	71.9/66.3	67.7/66.5	72.7/72.7	67.7/65.3
AUC	0.83	0.84	0.80	0.76	0.84	0.74
Hand-crafted feature						
Accuracy	79.8	80.5	70.3	69.8	80.5	68.1
Precision(0/1)	78.0/79.2	79.8/79.9	73.2/68.2	66.1/70.7	79.8/80.0	67.7/65.2
Recall(0/1)	75.0/85.1	76.5/85.1	66.9/77.7	75.3/64.1	77.7/84.7	66.2/70.7
F1 score(0/1)	78.6/79.4	78.4/79.9	66.8/68.6	68.6/64.9	79.0/79.6	70.1/66.1
AUC	0.84	0.85	0.81	0.74	0.86	0.75

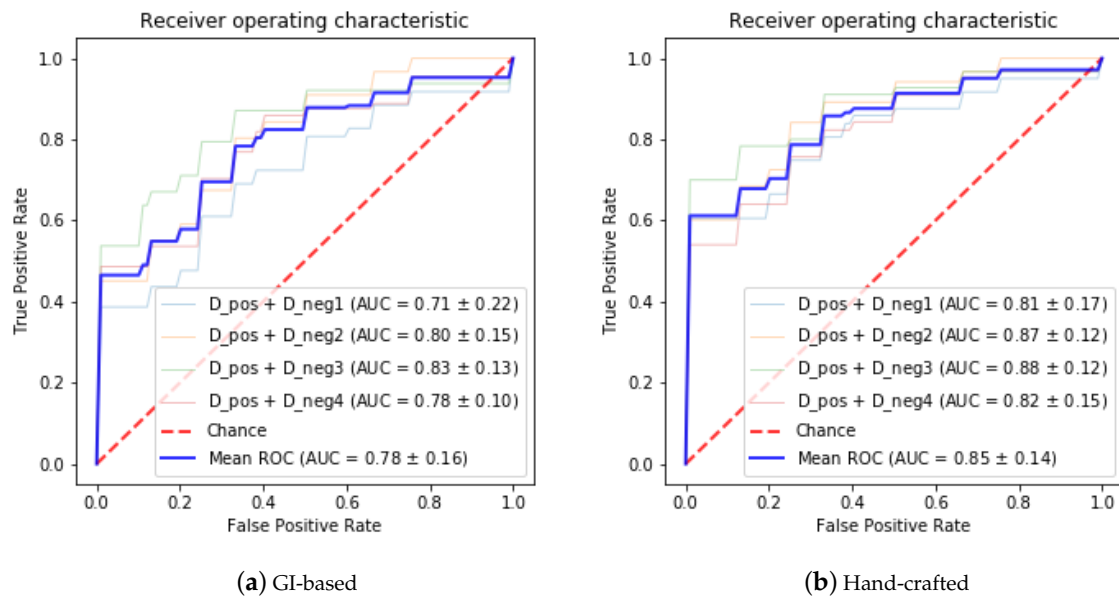


Figure 4. Receiver operating characteristic curves using Logistic regression.

4. Discussion

Of the five feature sets, hand-crafted features generally provided the best performance.

The eight-dimensional hand-crafted features include sex, HR_mean, remifentanil_CE_max, remifentanil_CP_max, remifentanil_VOL_max, remifentanil_VOL_mean, BIS_min, and MV_max. Each of the features was carefully chosen by intensive examination of the datasets, and we found that there have been studies that support the choices. For example, it was discovered that female patients were more likely to have arrhythmia than male patients, which supports the variable “sex” [24,25]. In [26], the heart rate feature was utilized to predict tachycardia, which supports the variable “HR_mean.” The four variables related to remifentanil are related to the fact that it may decrease heart rates [27,28] and that post-intubation tachycardia occurs more frequently in small dose patients than large dose patients [29]. The BIS values are known to be strongly related to prognoses in patients [30], which are related to the variable “BIS_min.” It has been discovered that respiration features, which are related to the variable ‘MV_max’, contribute to prediction of tachycardia [31].

One can argue that using all 153-dimensional features f_{input} must be better than other feature sets. More features might help improve performance, but they often fail when we do not balance model complexity and inherent data complexity. The total number of datasets for each experiment is close to 102, and the dimension of all features is 153. Such imbalance between them causes the machine learning models to overfit to a given training data; they will exhibit almost perfect performance only for the training data as shown in Figure 5. Note that we performed a grid search to find optimal parameter settings for every feature set. For example, the ANN model has an L2 penalty of 0.1, and the C value of SVM is 0.1 for f_{input} . The LR model appears not to be overfit, which may be related to the fact that the complexity of the LR model was successfully balanced by regularization. On the other hand, SVM and ANN were overfit, meaning that they were poorly generalized. Nonetheless, in terms of precision, the SVM with hand-crafted features outperformed the LR. In terms of recall, the ANN achieved the same performance as the LR. This implies that different models can be chosen for different purposes or requirements. In general, recall for tachycardia is the most important, so the LR with hand-crafted features will be optimal.

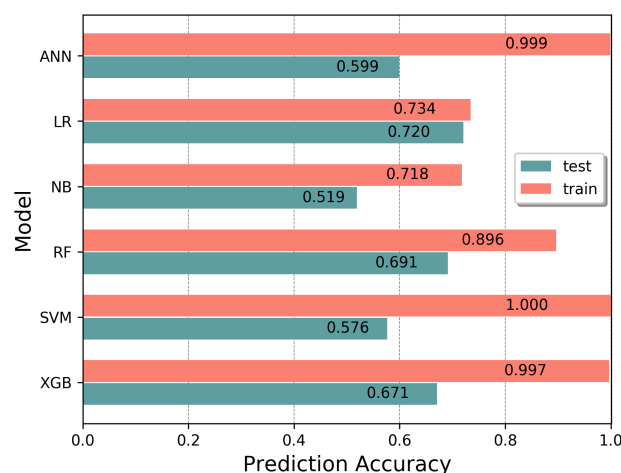


Figure 5. Accuracies with all features on training/test data.

This study is limited by its small dataset. Although the original number of collected datasets was 1931, we had only 257 patients data after filtering. As machine learning models learn from the dataset, we believe that performance will improve if more data are gathered. We will continue collecting more data to create better models.

5. Conclusions

In this paper, to predict post-intubation tachycardia, we compared five feature sets with various machine learning models. We collected datasets of two types (e.g., EMR and vital signs), and developed an algorithm to find intubation points due to annotation errors. The feature sets were defined using feature selection algorithms, statistical inspection, or manual examination. By experimental results, logistic regression (LR) model achieved the best accuracy and sensitivity with eight-dimensional hand-crafted features. To improve performance, more data should be collected and better models investigated. We will also perform further experiments with other different settings.

Author Contributions: Conceptualization, Y.-S.J.; data curation, A.R.K., W.J., Y.H.C., and B.S.K.; methodology, H.K.; software, W.J.; supervision, Y.-S.J. and S.H.K.; writing—original draft, H.K.; writing—review and editing, H.K., Y.-S.J., and S.H.K. All authors have read and agreed to the published version of the manuscript.

Funding: This research received no external funding.

Acknowledgments: This work was supported by the National Research Foundation of Korea(NRF) grant funded by the Korea government(MSIP; Ministry of Science, ICT & Future Planning) (No. 2019021348). This research was supported by the Soonchunhyang University Research Fund.

Conflicts of Interest: The authors declare no conflict of interest.

Appendix A

Table A1. Feature sets.

All 153 Features	RFE-Based	GI-Based	UST-Based	P-Based	Hand-Crafted
Age					
Sex					•
Height					
Weight					
BMI					
ASA classification					
Comorbidities - no.					
Cardiovascular disease					

Table A1. Cont.

All 153 Features	RFE-Based	GI-Based	UST-Based	P-Based	Hand-Crafted
Hypertension					
Atrial fibrillation					
Coronary artery disease					
Angina pectoris					
Congestive heart failure					
Respiratory disease					
Asthma					
COPD					
Gastrointestinal disease					
Hepatitis					
Liver cirrhosis					
Viral carrier					
Hepatitis B viral infection					
Renal disease					
Chronic kidney injury					
End-stage renal disease					
Endocrine disease					
Diabetes mellitus					
Thyroid disease					
Hemoglobin A1c			•		
Neurologic disease					
Cerebrovascular disease					
Dementia					
Baseline					
Systolic blood pressure					
Mean blood pressure					
Diastolic blood pressure					
Heart rate			•	•	
Noninvasive blood pressure					
Systolic					
Min					
Max					
Mean					
Sd					
Mean					
Min					
Max					
Mean					
Sd					
Diastolic					
Min					
Max					
Mean					
Sd					
Heart rate					
Min	•	•	•		
Max	•	•	•		
Mean	•	•	•	•	•
Sd	•				
Difference Heart rate					
Max		•			
Mean		•			
Sd					
Mechanical ventilation data					
Tidal volume					
Min					
Max					
Mean					
Sd					

Table A1. Cont.

All 153 Features	RFE-Based	GI-Based	UST-Based	P-Based	Hand-Crafted
Minute ventilation					
Min					
Max		•			•
Mean					
Sd					
Respiratory rate					
Min					
Max					
Mean					
Sd					
Mean positive airway pressure					
Min					
Max					
Mean					
Sd					
Peak inspiratory pressure					
Min					
Max					
Mean					
Sd					
End-tidal CO2 partial pressure					
Min					
Max			•		
Mean	•				
Sd					
Carbon dioxide					
Min					
Max					
Mean		•			
Sd					
PLETH_SPO2					
Min					
Max					
Mean	•				
Sd					
Positive endexpiratory pressure					
Min					
Max					
Mean					
Sd		•			
Neuromuscular transmission					
Mean of train-of-four count					
Bispectral Index					
Spectral frequency					
Min					
Max					
Mean		•			
Sd					
Signal quality index					
Min					
Max					
Mean					
Sd			•		
Electromyography					
Min		•			
Max					
Mean			•		
Sd					

Table A1. Cont.

All 153 Features	RFE-Based	GI-Based	UST-Based	P-Based	Hand-Crafted
Total power					
Min					
Max		•			
Mean	•	•			
Sd					
Bispectral index value					
Min			•		•
Max			•		
Mean					
Sd	•				
Anesthetic drug					
Volume					
Propofol					
Min		•			
Max					
Mean					
Sd					
Remifentanil					
Min					
Max					•
Mean				•	•
Sd					
Rate					
Propofol min					
Min					
Max					
Mean		•	•		
Sd	•				
Remifentanil min					
Min					
Max					
Mean					
Sd					
Plasma concentration					
Propofol min					
Min					
Max					
Mean					
Sd					
Remifentanil					
Min					
Max	•		•		•
Mean					
Sd					
Effect-site concentration					
Propofol					
Min		•			
Max					
Mean					
Sd					
Remifentanil					
Min					
Max					•
Mean			•		
Sd					
Target concentration					
Propofol min					
Min					
Max					

Table A1. Cont.

All 153 Features	RFE-Based	GI-Based	UST-Based	P-Based	Hand-Crafted
Mean					
Sd					
Remifentanil min					
Min					
Max					
Mean					
Sd					
Vasoactive drug administration					
Ephedrine					
Phenylephrine					
Esmolol					
Nicardipine					
Dexamethasone					
Muscle relaxant					
Rocuronium					
Pre-intubation sinus tachycardia					
Occurrence					•
Frequency					•
Duration of intubation					

RFE stands for recursive feature elimination, GI means Gini index, UST implies univariate statistical test, and P-based represents *p*-value based feature sets, COPD indicates chronic obstructive pulmonary disease, and PLETH_SPO2 means saturation of partial pressure of oxygen.

References

- Forbes, A.M.; Dally, F. Acute hypertension during induction of anaesthesia and endotracheal intubation in normotensive man. *BJA: Br. J. Anaesth.* **1970**, *42*, 618–624. [[CrossRef](#)]
- Watterson, L.; Morris, R.; Williamson, J.; Westhorpe, R. Crisis management during anaesthesia: Tachycardia. *BMJ Qual. Saf.* **2005**, *14*, e10. [[CrossRef](#)] [[PubMed](#)]
- Paix, A.; Runciman, W.; Horan, B.; Chapman, M.; Currie, M. Crisis management during anaesthesia: Hypertension. *BMJ Qual. Saf.* **2005**, *14*, e12. [[CrossRef](#)] [[PubMed](#)]
- Exner, D.V.; Reiffel, J.A.; Epstein, A.E.; Ledingham, R.; Reiter, M.J.; Yao, Q.; Duff, H.J.; Follmann, D.; Schron, E.; Greene, H.L.; et al. Beta-blocker use and survival in patients with ventricular fibrillation or symptomatic ventricular tachycardia: The Antiarrhythmics Versus Implantable Defibrillators (AVID) trial. *J. Am. Coll. Cardiol.* **1999**, *34*, 325–333. [[CrossRef](#)]
- Saito, S.; Nishihara, F.; Akihiro, T.; Nishikawa, K.; Obata, H.; Goto, F.; Yuki, N. Landiolol and esmolol prevent tachycardia without altering cerebral blood flow. *Can. J. Anesth.* **2005**, *52*, 1027. [[CrossRef](#)]
- Chen, A.; Ashburn, M.A. Cardiac effects of opioid therapy. *Pain Med.* **2015**, *16*, S27–S31. [[CrossRef](#)]
- Jeong, Y.S.; Kang, A.R.; Jung, W.; Lee, S.J.; Lee, S.; Lee, M.; Chung, Y.H.; Koo, B.S.; Kim, S.H. Prediction of Blood Pressure after Induction of Anesthesia Using Deep Learning: A Feasibility Study. *Appl. Sci.* **2019**, *9*, 5135. [[CrossRef](#)]
- Jovic, A.; Bogunovic, N. Evaluating and comparing performance of feature combinations of heart rate variability measures for cardiac rhythm classification. *Biomed. Signal Process. Control* **2012**, *7*, 245–255. [[CrossRef](#)]
- Ehtiati, N.; Attarodi, G.; Dabanloo, N.J.; Sedehi, J.F.; Nasrabadi, A.M. Prediction of ventricular tachycardia using nonlinear features of heart rate variability signal such as poincare plot, approximate and sample entropy, recurrence plot. In Proceedings of the 2017 Computing in Cardiology (CinC), Rennes, France, 24–27 September 2017; IEEE: Piscataway, NJ, USA, 2017; pp. 1–4.
- Shashikant, R.; Chetankumar, P. Predictive model of cardiac arrest in smokers using machine learning technique based on Heart Rate Variability parameter. *Appl. Comput. Inform.* **2019**. [[CrossRef](#)]

11. Joo, S.; Choi, K.J.; Huh, S.J. Prediction of ventricular tachycardia by a neural network using parameters of heart rate variability. In Proceedings of the 2010 Computing in Cardiology, Belfast, UK, 26–29 September 2010; IEEE: Piscataway, NJ, USA, 2010; pp. 585–588.
12. Riasi, A.; Mohebbi, M. Prediction of ventricular tachycardia using morphological features of ECG signal. In Proceedings of the 2015 The International Symposium on Artificial Intelligence and Signal Processing (AISP), Mashhad, Iran, 3–5 March 2015; IEEE: Piscataway, NJ, USA, 2015; pp. 170–175.
13. Yaghouby, F.; Ayatollahi, A.; Soleimani, R. Classification of cardiac abnormalities using reduced features of heart rate variability signal. *World Appl. Sci. J.* **2009**, *11*, 1547–1554.
14. Lee, H.C.; Jung, C.W. Vital Recorder—A free research tool for automatic recording of high-resolution time-synchronised physiological data from multiple anaesthesia devices. *Sci. Rep.* **2018**, *8*, 1527. [[CrossRef](#)] [[PubMed](#)]
15. Hira, Z.M.; Gillies, D.F. A review of feature selection and feature extraction methods applied on microarray data. *Adv. Bioinform.* **2015**, *2015*. [[CrossRef](#)] [[PubMed](#)]
16. Pedregosa, F.; Varoquaux, G.; Gramfort, A.; Michel, V.; Thirion, B.; Grisel, O.; Blondel, M.; Prettenhofer, P.; Weiss, R.; Dubourg, V.; et al. Scikit-learn: Machine learning in Python. *J. Mach. Learn. Res.* **2011**, *12*, 2825–2830.
17. Breiman, L. Random forests. *Mach. Learn.* **2001**, *45*, 5–32. [[CrossRef](#)]
18. Peng, C.Y.J.; So, T.S.H.; Stage, F.K.; John, E.P.S. The use and interpretation of logistic regression in higher education journals: 1988–1999. *Res. High. Educ.* **2002**, *43*, 259–293. [[CrossRef](#)]
19. Zhang, H. The optimality of naive Bayes. *AA* **2004**, *1*, 3.
20. Burges, C.J. A tutorial on support vector machines for pattern recognition. *Data Min. Knowl. Discov.* **1998**, *2*, 121–167. [[CrossRef](#)]
21. Chen, T.; Guestrin, C. Xgboost: A scalable tree boosting system. In Proceedings of the 22nd acm sigkdd international conference on knowledge discovery and data mining, San Francisco, CA, USA, 13–17 August 2016; pp. 785–794.
22. Haykin, S. *Neural Networks and Learning Machines, 3/E*; Pearson Education: Bengaluru, India, 2010.
23. Powers, D.M. Evaluation: From precision, recall and F-measure to ROC, informedness, markedness and correlation. *Mach. Learn. Technol.* **2011**, *2*, 37–63.
24. Tadros, R.; Ton, A.T.; Fiset, C.; Nattel, S. Sex differences in cardiac electrophysiology and clinical arrhythmias: Epidemiology, therapeutics, and mechanisms. *Can. J. Cardiol.* **2014**, *30*, 783–792. [[CrossRef](#)]
25. Villareal, R.P.; Woodruff, A.L.; Massumi, A. Gender and cardiac arrhythmias. *Tex. Heart Inst. J.* **2001**, *28*, 265.
26. Yoon, J.H.; Mu, L.; Chen, L.; Dubrawski, A.; Hravnak, M.; Pinsky, M.R.; Clermont, G. Predicting tachycardia as a surrogate for instability in the intensive care unit. *J. Clin. Monit. Comput.* **2019**, 1–13. [[CrossRef](#)] [[PubMed](#)]
27. Chanavaz, C.; Tirel, O.; Wodey, E.; Bansard, J.Y.; Senhadji, L.; Robert, J.C.; Ecoffey, C. Haemodynamic effects of remifentanyl in children with and without intravenous atropine. An echocardiographic study. *Br. J. Anaesth.* **2004**, *94*, 74–79. [[CrossRef](#)] [[PubMed](#)]
28. Thompson, J.; Hall, A.; Russell, J.; Cagney, B.; Rowbotham, D. Effect of remifentanyl on the haemodynamic response to orotracheal intubation. *Br. J. Anaesth.* **1998**, *80*, 467–469. [[CrossRef](#)] [[PubMed](#)]
29. Hogue, C.W.; Bowdle, T.A.; O’Leary, C.; Duncalf, D.; Miguel, R.; Pitts, M.; Streisand, J.; Kirvassilis, G.; Jamerson, B.; McNeal, S.; et al. A multicenter evaluation of total intravenous anesthesia with remifentanyl and propofol for elective inpatient surgery. *Anesth. Analg.* **1996**, *83*, 279–285. [[CrossRef](#)]
30. Stammet, P.; Werer, C.; Mertens, L.; Lorang, C.; Hemmer, M. Bispectral index (BIS) helps predicting bad neurological outcome in comatose survivors after cardiac arrest and induced therapeutic hypothermia. *Resuscitation* **2009**, *80*, 437–442. [[CrossRef](#)]
31. Lee, H.; Shin, S.Y.; Seo, M.; Nam, G.B.; Joo, S. Prediction of ventricular tachycardia one hour before occurrence using artificial neural networks. *Sci. Rep.* **2016**, *6*, 32390. [[CrossRef](#)]

